Precursors of catastrophe in the Bak-Tang-Wiesenfeld, Manna, and random-fiber-bundle models of failure

Srutarshi Pradhan* and Bikas K. Chakrabarti†
Saha Institute of Nuclear Physics, 1/AF Bidhan Nagar, Kolkata 700 064, India
(Received 6 July 2001; published 17 December 2001)

We have studied precursors of the global failure in some self-organized critical models of sandpile [in Bak-Tang-Wiesenfeld (BTW) and Manna models] and in the random-fiber-bundle model (RFB). In both BTW and Manna model, as one adds a small but fixed number of sand grains (heights) to any central site of the stable pile, the local dynamics starts and continues for an average relaxation time τ and an average number of topplings Δ spread over a radial distance ξ. We find that these quantities all depend on the average height h_{av} of the pile and they all diverge as h_{av} approaches the critical height h_c from below: $\Delta \sim (h_c - h_{av})^{-\delta}$, $\tau \sim (h_c - h_{av})^{-\gamma}$, and $\xi \sim (h_c - h_{av})^{-\nu}$. Numerically, we find $\delta \simeq 2.0$, $\gamma \simeq 1.2$, and $\nu \simeq 1.0$ for both BTW and Manna model in two dimensions. In the strained RFB model, we find that the breakdown susceptibility χ (giving the differential increment of the number of broken fibers due to increase in external load) and the relaxation time τ, both diverge as the applied load or stress σ approaches the network failure threshold σ_c from below: $\chi \sim (\sigma_c - \sigma)^{-1/2}$ and $\tau \sim (\sigma_c - \sigma)^{-1/2}$. These self-organized dynamical models of failure, therefore, show some definite precursors with robust power laws long before the failure point. Such well-characterized precursors should help predicting the global failure point of the systems in advance.

DOI: 10.1103/PhysRevE.65.016113 PACS number(s): 05.50.+q, 05.70.Ln, 05.65.+b, 05.40.−a

I. INTRODUCTION

In a sandpile, whenever the local slope at the surface of the pile exceeds the angle of repose, avalanches take place and the sand grains move to the neighboring sites. If the local slope of these neighboring sites increase, in turn, beyond the angle of repose, avalanches continue. Otherwise the dynamics stops until another sand grain is added to the pile. The system finally attains a self-organized state where extra grains, when added, get out of the system through successive avalanches from its boundary. Models of sandpiles have been developed to study such self-organization. Bak, Tang, and Wiesenfeld (BTW) [1,2] introduced the random height sandpile model, where height units are added randomly at any site at a constant rate and a site topples when its height equals an integer threshold value h_{th} ($=4$ for square lattice, for example). Whenever any site topples, the local height becomes zero there and the height is locally conserved by equal sharing among the nearest neighbors (four in number for square lattice) and the neighbors get one unit of height added to theirs'. The boundary of the system is completely absorbing. As more and more grains (heights) are added slowly to the system, the average height h_{av} of the system gradually increases and attains a critical height h_c (equivalent to the angle of repose of the sandpile), beyond which the growth of average height stops as the further addition of grains at any site causes successive avalanches or failures of all sizes. These happen due to the long-range correlations developed and the additional grains finally get out of the system through its boundaries. The self-organized state here becomes critical as it involves power law behavior in avalanche size distribution and the corresponding lifetime distribution. Extensive numerical checkings confirmed this self-organized critical behavior in both two- and three-dimensional sandpiles [3,4]. Later, Manna introduced [5] a two state and stochastic version of the BTW model, where the threshold height has been chosen to be two ($h_{th}=2$). The toppling at any site reduces the height there to zero and the toppled heights add to the height of any stocastically chosen site among the four neighboring sites of the toppled one. Here also, with constant addition of sand grains, the system gradually reaches again a critical state and there the avalanche size distribution and the corresponding lifetime distribution again follow similar scaling behavior. However, the exponents for the Manna model seem to be different [5,6] from those of the BTW model. A similar self-organizing dynamics is also seen in a strained random-fiber-bundle (RFB) model [7–12], where N fibers are connected in parallel to each other and clamped between their two ends. The strength of the individual fibers has a random distribution (white, Gaussian or otherwise). Under a load F, a fraction of the fibers fail immediately whose strengths are less than the stress $\sigma(=F/N)$. After this, the total load of the bundle redistributes globally as the stress is transferred from broken fibers to the remaining unbroken ones. This redistribution causes secondary failures that, in general, causes further failures and so on. After some typical relaxation time τ (dependent on σ), the system ultimately becomes stable if the applied stress σ is less than a critical value σ_c, beyond which all the fibers break and the network fails completely. Although the RFB model is not a self-organized critical one (as the failure state at $\sigma > \sigma_c$ is not critical), it has some self-organizing dynamics (stress redistribution for $\sigma \leq \sigma_c$) similar to the earlier ones and is very simple to tackle analytically. The studies of these self-organizing model systems and their scaling behavior have been extremely useful in analyzing the

*Email address: spradhan@cmp.saha.ernet.in
†Email address: bikas@cmp.saha.ernet.in

statistics of fracture and breakdown in real materials, including in earthquakes [4,13,14].

An obvious question arises: Are there any precursors or prior indications that can tell how far a (slowly) growing sandpile or a gradually strained fiber bundle is away from its global failure point? The study of precursors in self-organized systems was initiated by Acharyya and Chakrabarti [15]. Here, the global failure is identified as the system spanning avalanche occurring at $h_{av}=h_c$. They tried to study the response of BTW model to pulsed addition of grains (heights) in two- and three-dimensional sandpiles, where "pulse" means a fixed number of grains, added at any site to trigger the dynamics locally in time and space. Adding a pulse of heights at any site of a stable pile (where toppling had stopped), they measured the response of the system in terms of the number of affected or toppled sites (Δ) and the corresponding response or relaxation time (τ) at various average heights (h_{av}) of the system. They observed that both Δ and τ diverge as h_{av} approaches the critical height h_c. They also estimated the exponents involved in the power laws for these divergences. However, these estimates for the exponent values were not quite accurate due to the small system sizes considered and strong pulses applied. Similarly, the breakdown susceptibility [15] of the RFB model was studied by measuring the increment in the number of broken fibers with the increment in the stress σ [16]. It was seen that this differential increase in the number of broken fibers due to infinitesimal increase in stress σ, diverges as the stress σ approaches the global failure threshold σ_c.

In this paper, we have studied several precursors in the models of sandpiles and random-fiber-bundle. We have studied the response of sandpile models (both BTW and Manna model) to pulsed addition of sand grains (heights; for unit time or unit pulse width), where the applied pulse strength is negligible, so that the statistical state of the system is not perturbed significantly by the applied pulse. We have identified three parameters, namely, the total number of topplings (Δ), the corresponding relaxation time (τ), and the correlation length (ξ); all of which diverge as the average height (h_{av}) of the pile approaches the critical height (h_c). The values of the exponents for the variations of these quantities (Δ, τ, and ξ) with h_{av} near h_c have been estimated accurately. In fact, the estimated value of the critical height or the location of the catastrophe point h_c, extrapolated separately from the growing (precursor) values of Δ, τ, and ξ (for h_{av} values below h_c), agree quite well with the previous direct numerical estimates [17] for the same. In the RFB model, we have studied the breakdown susceptibility (χ) and the response time (τ) required for the bundle to become stable when an initial load or stress σ ($<\sigma_c$) is applied on it. Both χ and τ diverge as σ approaches σ_c. The growth behavior of these precursors for σ below σ_c and the possibility of their extrapolations for estimating the failure point σ_c of the network is discussed.

II. PRECURSORS IN THE BTW MODEL

A. Model

Let us consider a BTW model on a square lattice of size $L\times L$. At each lattice site (i,j) there is an integer variable $h_{i,j}$, which represents the height of the sand column at that site. A unit of height (one sand grain) is added at a randomly chosen site at each time step and the system evolves in discrete time. The dynamics starts as soon as any site (i,j) has got a height equal to the threshold value ($h_{th}=4$): the site topples, i.e., $h_{i,j}$ becomes zero there, and the heights of the four neighboring sites increase by one unit

$$h_{i,j}\rightarrow h_{i,j}-4,\ \ h_{i\pm1,j}\rightarrow h_{i\pm1,j}+1,\ \ \text{and}\ \ h_{i,j\pm1}\rightarrow h_{i,j\pm1}+1. \tag{1}$$

If, due to this toppling at site (i,j), any neighboring site become unstable (its height reaches the threshold value) they, in turn, follow the same dynamics. The process continues till all sites become stable [$h_{i,j}<h_{th}$ for all (i,j)]. When toppling occurs at the boundary of the lattice (four nearest neighbors are not available), extra heights get off the lattice and are removed from the system.

With a very slow but steady rate of addition of unit height (sand grain) at random sites of the lattice, the avalanches get correlated over longer and longer ranges and the average height (h_{av}) of the system grows with time. Gradually, the correlation length (ξ) becomes of the order the system size L. Here, on average, the additional height units start leaving the system as the system approaches toward a critical average height $h_c(L)$ and the average height remains stable there (see Fig. 1). Also the system becomes critical here as the distributions of the avalanche sizes and the corresponding lifetimes follow robust power laws [3,4]. In fact, a finite size scaling fit $h_c(L)=h_c(\infty)+CL^{-1/\nu}$ [obtained by setting $\xi\sim|h_c(L)-h_c(\infty)|^{-\nu}=L$], where C is a constant, with $\nu\simeq1.0$ gives $h_c\equiv h_c(\infty)\simeq2.124$ (see inset of Fig. 1). Similar finite size scaling fit with $\nu=1.0$ gave $h_c(\infty)\simeq2.124$ in earlier large scale simulations [17].

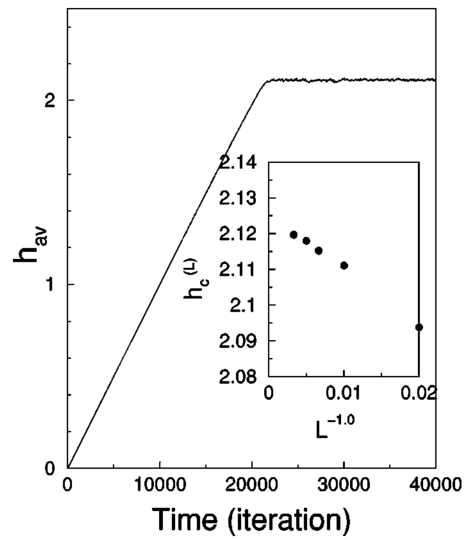

FIG. 1. The growth of average height h_{av} [$<h_c(L)$] of the BTW model against the number of iterations of adding unit heights ($L=100$). In the inset, we show the finite size behavior of the critical height $h_c(L)$, obtained from simulation results for different L.

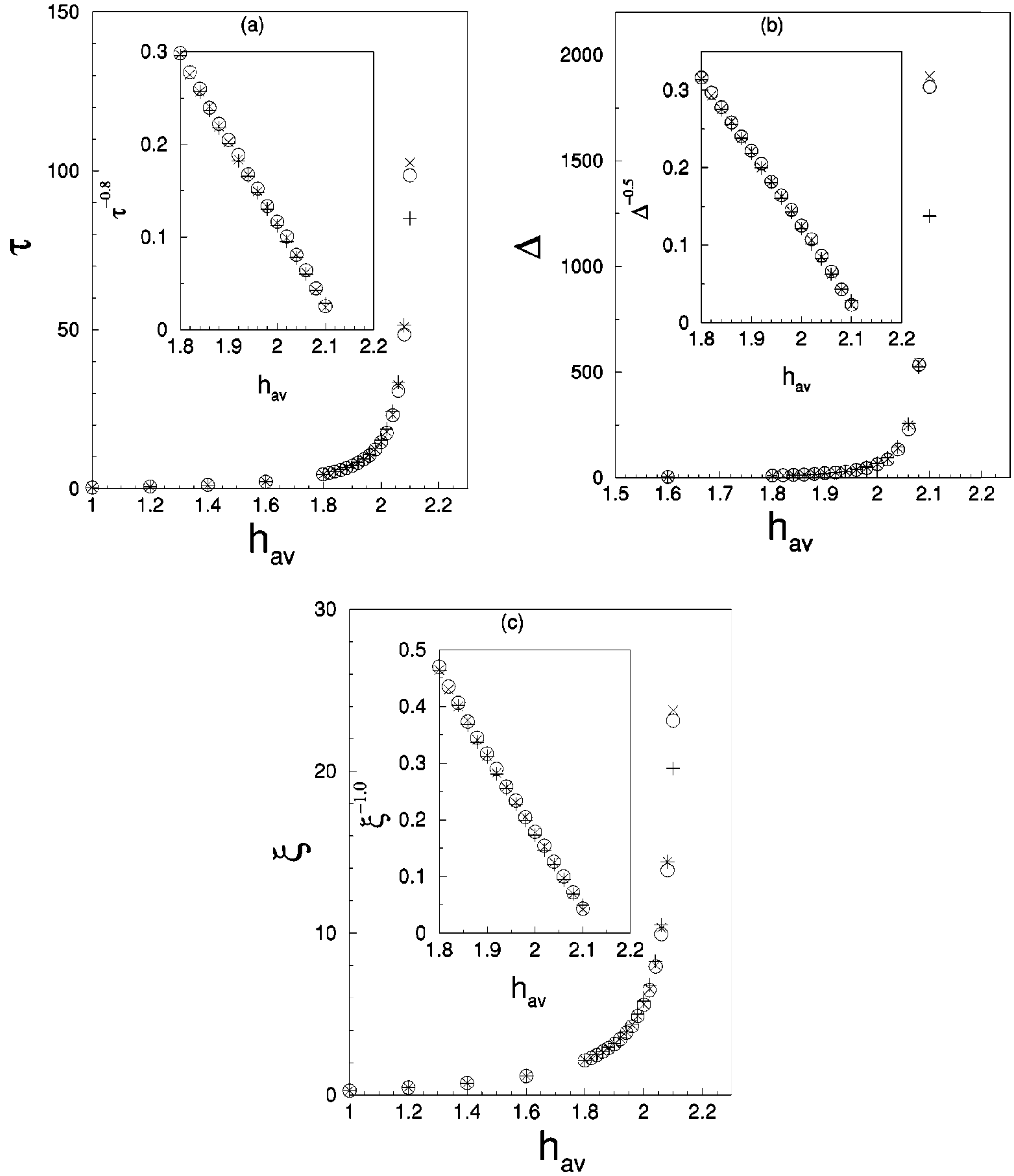

FIG. 2. The variations of the precursors with h_{av} $[<h_c(L)]$ in the BTW model for different system sizes: $L=100$ (plus), $L=200$ (cross), and $L=300$ (open circle). (a) For relaxation time τ; in the inset $\tau^{-0.8}$ is plotted against h_{av}. (b) For the total number of topplings Δ; inset shows $\Delta^{-0.5}$ vs h_{av} plot. (c) For the correlation length ξ; in the inset, $\xi^{-1.0}$ is plotted against h_{av}.

B. Simulation studies for pulsed perturbation

We have taken random height BTW systems on square lattice of different sizes ($L=100$, 200, and 300). At a fixed value of L, for any pile configuration at an average height h_{av}, when all sites of the system have become stable (dynamics have stopped), a fixed number of height units $h_p=4$ (pulse of sand grains) is added at any central point of the system. Just after this addition, the local dynamics starts and it takes a finite time or iterations to return back to the stable state $[h_{i,j}<4$ for all $(i,j)]$ after several toppling events. For each value of $h_{av}(<h_c)$, we take about 10^5 initial configurations and this response or relaxation time has been noted for each of them. The average relaxation time τ is obtained taking averages over all configurations and is seen to diverge as h_{av} approaches the critical height h_c [see Fig. 2(a)]. Near h_c, τ follows a power law $\tau\sim(h_c-h_{av})^{-\gamma}$, where $\gamma\cong1.2$. The plot of $\tau^{-1/\gamma}$ with h_{av} is a straight line with negative slope. Extrapolating the straight line and locating the vanishing point of $\tau^{-1/\gamma}$ one can estimate the critical point $h_c=2.13\pm.01$ [see inset of Fig. 2(a)] that is very close to the previous numerical estimate $h_c\cong2.124$ [17].

Another response parameter, the average size of the damage (Δ), i.e., the average number of topplings (after the addition of pulse) has been measured as follows: the number of topplings for each configuration at each value of h_{av} is noted and averaged out over the initial configurations (about 10^5 in number). Thus, the average Δ for that value of h_{av} is estimated and this is also seen to diverges as $h_{av}\to h_c$ [see Fig.

2(b)]. Near the critical point, we find $\Delta \sim (h_c - h_{av})^{-\delta}$, where $\delta \cong 2.0$. The plot of $\Delta^{-1/\delta}$ vs h_{av} gives a straight line with negative slope [see inset of Fig. 2(b)] that can again be used to estimate h_c $(=2.12 \pm .01)$ after extrapolating the straight line up to the vanishing point of $\Delta^{-1/\delta}$.

We have also measured the correlation length ξ of the system during the same experiment. When the pulse is added at any central point (i_0, j_0) of the system at some h_{av}, toppling starts there and gradually it moves toward the boundaries . We have marked the farthest affected site (i_f, j_f) (where at least one toppling has occurred due to the pulse) with respect to the central site (i_0, j_0) where the pulse had been added. Clearly, the average (over configurations) distance between the central and the farthest affected sites $(|(i_0, j_0) - (i_f, j_f)|)$ is a measure of the correlation length of the system at that h_{av}. This correlation length ξ is seen to diverge as $h_{av} \rightarrow h_c$ [see Fig. 2(c)] following a power law $\xi \sim (h_c - h_{av})^{-\nu}$, where $\nu \cong 1.0$. The plot of $\xi^{-1/\nu}$ vs h_{av} [see inset of Fig. 2(c)] is a straight line. The vanishing point of $\xi^{-1/\nu}$ gives an estimate of the critical point h_c and we find $h_c = 2.13 \pm 0.01$. This is also close to the previously estimated critical value.

III. PRECURSORS IN THE MANNA MODEL

A. Model

We consider now the Abelian Manna model on a square lattice of size $L \times L$, where the sites can be either empty or occupied with unit height i.e., the height variables can have binary states $h_{i,j} = 1$ or $h_{i,j} = 0$. A site is chosen randomly and one height is added at that site. If the site is initially empty, it gets occupied

$$h_{i,j} \rightarrow h_{i,j} + 1. \qquad (2)$$

If the chosen site is previously occupied then a toppling or "hard core interaction" rejects both the heights from that site

$$h_{i,j} \rightarrow h_{i,j} - 2 \qquad (3)$$

and each of these two rejected heights stochastically chooses its host among the four neighbors of the toppled site. The toppling can happen in chains if any chosen neighbor was previously occupied and thus cascades are created. After the system attains stable state (dynamics stopped), a new site is chosen randomly and unit height is added to it. Thus, the system evolves in discrete time steps. Here again, the boundary is assumed to be completely absorbing so that heights can leave the system due to the toppling at the boundary.

With a slow rate of addition of heights at random sites, initially the average height of the system grows with time and soon the system approaches toward a critical average height h_c, where the average height stabilizes and does not change with further addition of heights (see Fig. 3). The critical average height h_c has a finite size dependence and a similar finite size scaling fit $h_c(L) = h_c(\infty) + CL^{-1/\nu}$ gives $\nu \simeq 1.0$ and $h_c \equiv h_c(\infty) \simeq 0.716$ (see inset of Fig. 3). This is close to an earlier estimate $h_c \simeq 0.71695$ [18], made in a somewhat different version of the model. The avalanche size distribution has got power laws similar to the BTW model, at this self-organized critical state at $h_{av} = h_c$. However, the exponents seem to be different [5,6], compared to those of BTW model, for this stochastic model.

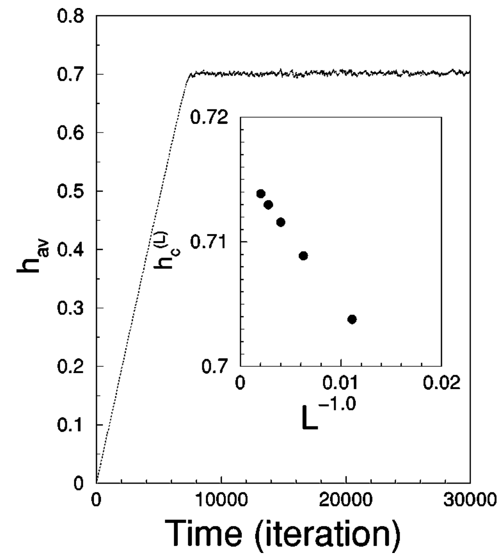

FIG. 3. The growth of average height h_{av} $[<h_c(L)]$ of the Manna model against the number of iterations of adding unit heights $(L=100)$. In the inset, we show the finite size dependence of the critical height $h_c(L)$, obtained from simulation results for different L.

B. Simulation studies with pulsed perturbation

We have considered Manna model on square lattice of different sizes ($L = 100$, 200, and 300). At a fixed value of L, for any pile configuration at an average height h_{av}, a fixed number of heights $h_p = 2$ has been added at any central point of the stable pile (for which dynamics had stopped). Just after the addition, the local dynamics starts and it takes a finite time (iteration number) to return back to the stable state $[h_{i,j} < 2$ for all $(i,j)]$ after several toppling events. For each value of $h_{av} (< h_c)$ this response time for each pile configuration has been noted and the average relaxation time τ is obtained from the average over 10^5 different configurations. Near critical point τ is seen to diverge [see Fig. 4(a)] as h_{av} approaches the critical height h_c with a power law $\tau \sim (h_c - h_{av})^{-\gamma}$, where $\gamma \cong 1.2$. The plot of $\tau^{-1/\gamma}$ with h_{av} is a straight line [see inset of Fig. 4(a)] with negative slope. Extrapolating the straight line and locating the vanishing point of $\tau^{-1/\gamma}$, we have estimated the critical height as $h_c = 0.72 \pm 0.01$, which is very close to the previous numerical estimate $h_c \cong 0.716$ for this model (see inset of Fig. 3).

The size of the damage, i.e., the total number of topplings (after the addition of pulse) has also been measured for the above cases. The average (over about 10^5 configurations) number of topplings Δ also diverges as average height h_{av} approaches the critical height h_c and near critical point Δ grows as $\Delta \sim (h_c - h_{av})^{-\delta}$, where $\delta \cong 2.0$ [see Fig. 4(b)]. The plot of $\Delta^{-1/\delta}$ vs h_{av} gives a straight line that can be used to estimate $h_c (= 0.72 \pm 0.01)$ after extrapolation [see inset of Fig. 4(b)].

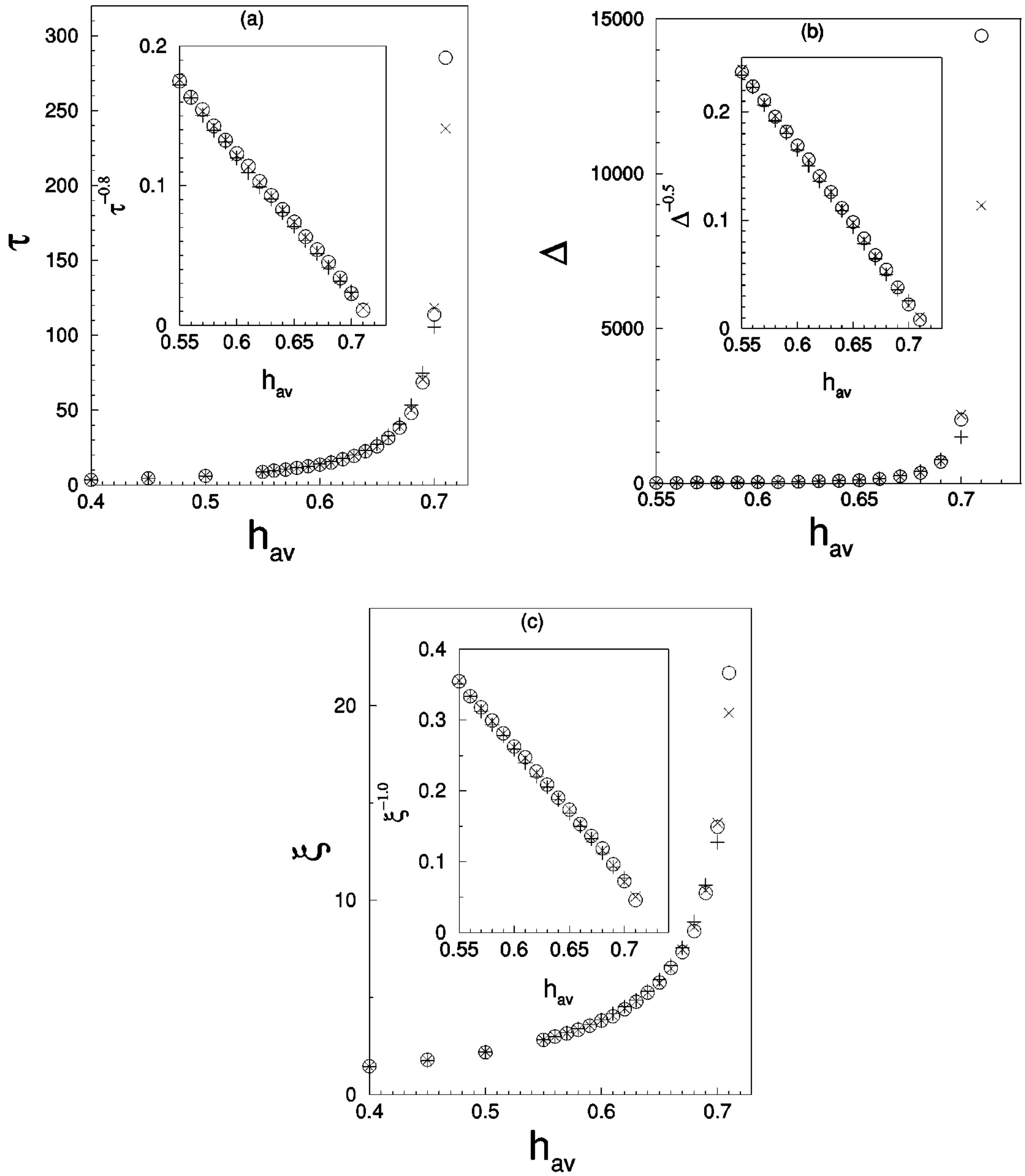

FIG. 4. The variations of the precursors with h_{av} $[<h_c(L)]$ in the Manna model for different system sizes: $L=100$ (plus), $L=200$ (cross), and $L=300$ (open circle). (a) For relaxation time τ; in the inset $\tau^{-0.8}$ is plotted against h_{av}. (b) For the total number of topplings Δ; inset shows $\Delta^{-0.5}$ vs h_{av} plot. (c) For the correlation length ξ; in the inset, $\xi^{-1.0}$ is plotted against h_{av}.

The correlation length (ξ) of the system has been measured following the same procedure as in the BTW model, described in the previous section. The average (over about 10^5 configurations) correlation length ξ again diverges [see Fig. 4(c)] as $h_{av}\to h_c$ and near critical point ξ follows the power law $\xi \sim (h_c - h_{av})^{-\nu}$, where $\nu \cong 1.0$. The plot of $\xi^{-1/\nu}$ vs h_{av} is a straight line with negative slope and the vanishing value of $\xi^{-1/\nu}$ estimates the critical density $h_c = 0.72 \pm 0.01$ [see inset of Fig. 4(c)] that is again close to the estimated critical density from direct numerical study.

IV. PRECURSORS IN THE RANDOM-FIBER-BUNDLE MODEL

A. The model

We consider a RFB model containing N elastic fibers clamped at two ends, where the failure stress of the individual fibers are distributed randomly and uniformly within 0 and 1 (white distribution). Global load sharing is assumed and the applied load on the bundle is democratically shared among the existing intact fibers of the bundle. With the application of any small load F ($=\sigma N$, with $\sigma \ll 1$) on the bundle, an initial stress σ sets in. At the first step, σN number of fibers are broken off, leaving $Nu_1(\sigma)=(1-\sigma)N$ number of unbroken fibers. After this, the applied force is redistributed uniformly among remaining intact fibers and the stress (per fiber) is then readjusted to a value $F/[Nu_1(\sigma)]=\sigma/(1-\sigma)$. With this new readjusted stress, some extra fibers for which the strengths are below the above readjusted stress fail and the total number of broken fibers increases to a value $N[\sigma/(1-\sigma)]$, leaving $Nu_2(\sigma)=[1-\sigma/(1-\sigma)]N$ unbroken fibers. This, in turn, readjusts the stress again and induces further failure giving rise to a recursive relation

$$u_n(\sigma)=1-\frac{\sigma}{u_{n-1}(\sigma)} \tag{4}$$

for the fraction u of unbroken fibers at the nth and $(n-1)$th iteration for stress σ. This dynamics of successive failure propagates, therefore, in (discrete) time until $Nu_{n-1}(\sigma)-Nu_n(\sigma)\leqslant 1$, or the successive stress readjustments make so little change that even one fiber cannot be found in the network having strength between the successive readjusted value. For an infinite ($N\to\infty$) fiber bundle, we denote the fraction of unbroken fibers here by the fixed point value $u^*(\sigma)$. The critical stress σ_c is determined by that σ above which there is no fixed point and $u_n(\sigma)\to 0$ as $n\to\infty$. Because of the above simple recursion relation (4) for u, in the uniformly distributed RFB model, we can easily analyze the asymptotic features of its dynamics. The differential form of the above recursion relation (4) can be written as

$$\frac{du}{dn}=-\frac{(u^2-u+\sigma)}{u}. \tag{5}$$

The fixed point value of u is obtained by setting $du/dn=0$. This gives

$$u^*=\frac{1}{2}+(\sigma_c-\sigma)^{1/2}, \tag{6}$$

where $\sigma_c=1/4$. The other root is neglected here as it is unstable [see Eq. (7)]. Expanding the Eq. (5) near the fixed point value (6) of u, we can write $u=u^*+\epsilon$, and

$$\frac{d\epsilon}{dn}=-\frac{\epsilon(2u^*-1)}{u^*}\simeq-\epsilon[4(\sigma_c-\sigma)^{1/2}] \tag{7}$$

as $\sigma\to\sigma_c$, which gives

$$u_n=u^*+\text{const}\times\exp(-n/\tau_0), \tag{8}$$

where

$$\tau_0=\frac{1}{4}(\sigma_c-\sigma)^{-1/2}. \tag{9}$$

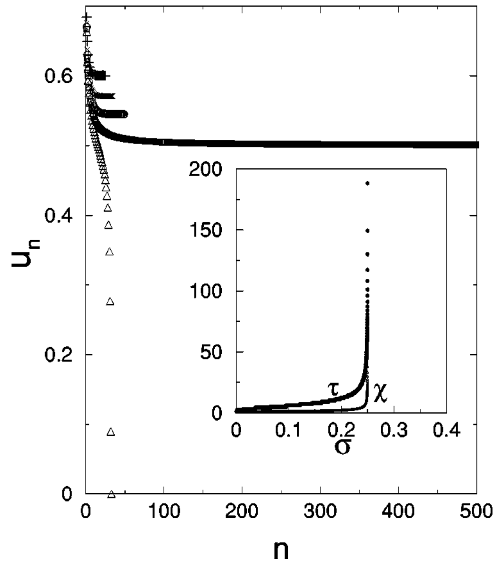

FIG. 5. Fraction of the unbroken fibers u_n at different times or iterations n in a RFB model with uniform strength distribution, for different values of (initial) stress: $\sigma=0.24$ (plus), $\sigma=0.245$ (cross), $\sigma=0.248$ (open circle), $\sigma=0.25$ (open square), and $\sigma=0.252$ (open triangle). Note that the last value of σ is greater than $\sigma_c(=1/4)$, and the fraction of unbroken fibers goes to zero here. Inset shows how the susceptibility χ (up triangle) and the relaxation time τ (filled circle) both diverge as $\sigma\to\sigma_c(=1/4)$.

B. Study of the precursors

We have simulated the RFB model with a very slow but steady increase of initial stress σ on a bundle containing N fibers ($N\sim 10^8$). Application of some small initial stress σ ($=F/N$) triggers the dynamics by breaking off a fraction $(1-u_n)$ of fibers, and global readjustment of the stress causes further failures ($u_{n+1}<u_n$). As mentioned before, after a few steps or iterations, when $N[u_{n-1}(\sigma)-u_n(\sigma)]\leqslant 1$, the dynamics stops and the bundle becomes stable. We note this relaxation time τ required for the stabilization. For each (initial) stress σ, we start afresh with the intact bundle and note the relaxation time for each σ. The observation continues until we reach the threshold stress σ_c ($=1/4$), above which the bundle fails totally (see Fig. 5). The relaxation time τ is seen to diverge as $\sigma\to\sigma_c$ following a power law $\tau\sim\tau_0\sim(\sigma_c-\sigma)^{-1/2}$ (see inset of Fig. 5) that can be explained easily using Eq. (8).

Similar studies have been made for the breakdown susceptibility $\chi\equiv dm/d\sigma$, where $m=N[1-u^*(\sigma)]$ is the total number of fibers broken finally by stress σ (see inset of Fig. 5). One finds $\chi\sim(\sigma_c-\sigma)^{-1/2}$, in agreement with the previous observations [11,16]. This can be easily explained from solution (6).

V. SUMMARY AND CONCLUDING REMARKS

In all the three dynamical models of failure we have considered here, we find that long before the occurrence of global failures, the growing correlations in the dynamics of constituent elements manifest themselves as various precursors. The number of topplings Δ, relaxation time τ, and the correlation length ξ, in both BTW and Manna model, grow and diverge following power laws as the systems approach their respective critical points h_c from below: $\Delta \sim (h_c - h_{av})^{-\delta}$, $\tau \sim (h_c - h_{av})^{-\gamma}$, and $\xi \sim (h_c - h_{av})^{-\nu}$. For two-dimensional systems, we find numerically here $\delta \simeq 2.0$, $\gamma \simeq 1.2$, and $\nu \simeq 1.0$ for both BTW and Manna model. We could not thus detect any significant difference in the power laws for these precursors. We also could not detect any significant finite size effect in these precursors. Though this size independence of the quantities we studied look quite unnatural at first sight, there are strong reasons. Basically, we study the behavior for $h_{av} < h_c$, the precursor behavior, where ξ is necessarily finite. As we add here the tiny pulse at some central site of a relatively large system, the boundary effect cannot be really felt because of the smallness of ξ compared to L for most values of h_{av}. This explains the lack of finite size effect in our precursor studies [which, of course, is clearly manifest when we check our model results at $h_{av} = h_c(L)$]. It may also be noted that since for h_{av} near h_c, in our system, ξ becomes of the order of L, at $h_{av} = h_c(L)$, our result suggests $\Delta \sim L^{2.0}$ and $\tau \sim L^{1.2}$. This, in fact, supports the earlier analytic result for $h_{av} = h_c(L)$ for large but finite systems, as obtained by Dhar [19]. Generally, if we write $\Delta \sim \xi^{d_f}$, we then get $d_f = \delta/\nu \simeq 2.0$ for the fractal dimension of the avalanche clusters.

Apart from the previous attempts [15], an indirect study in the fixed energy sand-pile (FES) model [18] also indicated similar power law behavior away from the critical point (essentially for h_{av} above h_c). In the BTW-FES model, the observed exponent values for τ and ξ differ significantly from those of ours'. However, for the Manna-FES model, these exponent values are close to our estimates. The FES version of the models are somewhat different by construction and the discrepancies in case of BTW-FES estimates (compared to ours') seem to be physical in their origin. Due to lack of stochasticity, BTW model can stabilize in several "metastable" states (above h_c) and nonuniversality occurs because of different initial conditions. This can also be seen from the difference in the estimate of the critical point h_c in the BTW and BTW-FES models; as mentioned before, no such difference in the h_c estimate seems to exist for the Manna and Manna-FES models. This difference in the h_c values for the BTW case might explain the difference in the exponent values we obtained (for $h_{av} < h_c$) and those obtained for the corresponding FES model (for $h_{av} > h_c$).

For the random-fiber-bundle model, we find that the breakdown susceptibility χ (giving the increment in the number of broken fibers for an infinitesimal increment of load on the network) and the corresponding relaxation time τ (required for the network to stabilize, after successive failures of the fibers), both diverge as the external load or stress approaches its global failure point σ_c from below: $\chi \sim (\sigma_c - \sigma_{av})^{-1/2}$ and $\tau \sim (\sigma_c - \sigma_{av})^{-1/2}$. These results for the RFB model are, of course, analytically derived here for uniform distribution of strength of the fibers. It may be mentioned here that a similar behavior for the time-to-fracture (for σ above σ_c; diverging with the same exponent 1/2 for τ) was observed in a RFB model, where the fibers relax, under stress, to the elastic strain through viscous damping [20]. However, the relaxational dynamics in this visco-elastic RFB model is not due to the (self-organizing) stress redistributions among the surviving fibers and, as such, is quite different in its origin. In fact, this time-to-failure vanishes in the limit of zero damping coefficient [20]. However, the similarities in the behavior in such distinctly different situations also indicate interesting possibilities.

Knowledge of the precursors and their power laws should help estimating precisely the location of the global failure or critical point from the proper extrapolation of the above quantities, which are available long before the failure occurs. The usefulness of such precursors can hardly be overemphasized.

ACKNOWLEDGMENTS

We are grateful to P. Bhattacharyya, A. Chakraborti, R. Karmakar, F. Kun, S. S. Manna, and A. Vespignani for useful comments, suggestions, and discussions.

[1] P. Bak, C. Tang and K. Wiesenfeld, Phys. Rev. Lett. **59**, 381 (1987).
[2] P. Bak, C. Tang and K. Wiesenfeld, Phys. Rev. A **38**, 364 (1988).
[3] P. Grassberger and S.S. Manna, J. Phys. (France) **51**, 1077 (1990).
[4] P. Bak, *How Nature Works* (Oxford University Press, Oxford, 1997).
[5] S.S. Manna, J. Phys. A **24**, L363 (1991).
[6] D. Dhar, Physica A **270**, 69 (1999).
[7] H.E. Daniels, Proc. R. Soc. London, Ser. A **183**, 405 (1945).
[8] P.C. Hemmer and A. Hansen, J. Appl. Mech. **59**, 909 (1992).
[9] A. Hansen and P.C. Hemmer, Phys. Lett. A **184**, 394 (1994).
[10] D. Sornette, J. Phys. I **2**, 2089 (1992).
[11] R. da Silveria, Am. J. Phys. **67**, 1177 (1999).
[12] Y. Moreno, J.B. Gomez, and A.F. Pacheco, Phys. Rev. Lett. **85**, 2865 (2000).
[13] B.K. Chakrabarti and L.G. Benguigui, *Statistical Physics of Fracture and Breakdown in Disorder Systems* (Oxford University Press, Oxford, 1997).
[14] D.L. Turcotte, Rep. Prog. Phys. **62**, 1377 (1999).
[15] M. Acharyya and B.K. Chakrabarti, Physica A **224**, 254 (1996); Phys. Rev. E **53**, 140 (1996).
[16] S. Zapperi, P. Ray, H.E. Stanley and A. Vespignani, Phys. Rev. Lett. **78**, 1408 (1997).
[17] S.S. Manna, J. Stat. Phys. **59**, 509 (1990).
[18] A. Vespignani, R. Dickman, M.A. Munoz, and S. Zapperi, Phys. Rev. E **62**, 4564 (2000); A. Chessa, E. Marinari, and A. Vespignani, Phys. Rev. Lett. **80**, 4217 (1998).
[19] D. Dhar, Physica A **186**, 82 (1992); *ibid.* **263**, 4 (1999).
[20] R.C. Hidalgo, F. Kun, and H.J. Herrmann, e-print cond-mat/0103232.